UDC 519.68:517.9
Original scientific paper
Received: 07.01.2002.

Two-dimensional BEM for analysis of potential Laplace problems

Slavko Vujević[(1)], **Višnja Srzentić-Gazzari**[(2)] and **Sergio Gazzari**[(2)]
[(1)]Faculty of Electrical Engineering, Mechanical Engineering and Naval Architecture, University of Split, Ruđera Boškovića bb, HR-21000 Split, CROATIA
e-mail: vujevic@fesb.hr
[(2)]Croatian National Electricity, Gundulićeva 42, HR-21000 Split, CROATIA

SUMMARY

The algorithm for two-dimensional (2D) boundary element method (BEM) analysis of potential Laplace problems with heterogeneous domain has been presented in this paper. Using double and multiple global node technique, the correct numerical approximation of the normal flux density at the points with its physically discontinuity has been made possible. The resulting system of linear equations has been extended by employing an additional set of linear equations. These equations are obtained by equalizing the potentials at concurrent global nodes. The procedure accuracy has been additionally increased using the new expressions obtained by analytical integration along the linear boundary elements. One example with analytical solution illustrates the developed algorithm.

***Key words**: 2D BEM analysis, potential Laplace problem, analytical integration, multiple global node technique.*

1. INTRODUCTION

Application of the BEM to the 2D potential Laplace problems has some numerical problems. One of them is accuracy of the numerical integration along the boundary elements. Therefore, in this paper, for linear boundary elements, the algorithm for exact analytical integration is developed. Furthermore the variation of the characteristics of the medium impose the division of the domain in several sub-domains. The division of the domain into sub-domains leads to special numerical problems at the intersection points of several interfaces (internal boundaries). Similar problems occur at all points in which discontinuity of the normal flux density must be satisfied. Several methods have been suggested to overcome the numerical problems at the intersection points [1]. These problems are successfully solved in this paper.

Advanced numerical procedure has been successfully applied for numerical analysis of the influence of the additional substance in the trench on earthing grid parameters [2].

2. APPLICATION OF THE BEM TO 2D POTENTIAL LAPLACE PROBLEM

We assume that heterogeneous domain Ω is divided into homogeneous and isotropic sub-domains Ω_i (Figure 1). The second assumption is that the unitary normal vector to the interface between two sub-domains has direction from sub-domain p to sub-domain q, where $p \leq q$.

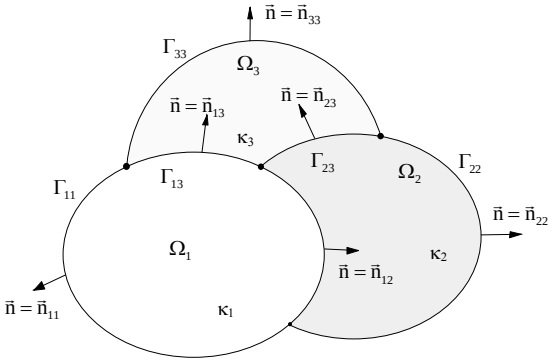

Fig. 1 Heterogeneous domain divided into three homogeneous sub-domains

The boundary conditions corresponding to this problem are of two types:

a) $\varphi = \overline{\varphi}$ on Γ_φ - Dirichlet boundary condition,

b) $q = \overline{q}$ on Γ_q - Neumann boundary condition,

where φ is the potential, q is the normal flux density and $\Gamma_\varphi \cup \Gamma_q$ is the boundary of the whole domain Ω.

2.1 Potential distribution equation

The potential φ_k at the point P_k (x_k, y_k), which is located within sub-domain Ω_p or on its boundary, is described by the following expression:

$$C_k \cdot \varphi_k = \sum_{r=1}^{NSD} a_{pr} \cdot \int_{\Gamma_{pr} \setminus P_k} \left(\frac{\psi_k \cdot q}{\kappa_p} - \varphi \cdot \frac{\partial \psi_k}{\partial n} \right) \cdot d\Gamma \quad (1)$$

where C_k is the constant [3] which depends on the position of the point P_k, NSD is the total number of sub-domains,

$$a_{pr} = \begin{cases} 1 & if \quad p \le r \\ 0 & if \ there \ is \ no \ interface \ \Gamma_{pr} \\ -1 & if \quad p > r \end{cases}$$

is the constant depending on the normal $\vec{n}_{pr}$ direction (Figure 1),

$$q = \begin{cases} \kappa_p \cdot \dfrac{\partial \varphi}{\partial n} & if \quad p \le r \\ \kappa_r \cdot \dfrac{\partial \varphi}{\partial n} & if \quad p > r \end{cases}$$

is the flux density along normal vector $\vec{n}_{pr}$, κ_p and κ_r are material conductivities,

$$\Psi_k = \frac{1}{2 \cdot \pi} \cdot ln \frac{1}{\sqrt{(x - x_k)^2 + (y - y_k)^2}} + A \quad (2)$$

is fundamental solution of the Poisson equation, where:

$$A = \frac{1}{2\pi} ln 100 \cdot d_{max}$$

is the constant which has been introduced to improve numerical stability of the algorithm, and d_{max} is the maximal distance between the nodes of the boundary element grid.

2.2 Discretization

Linear boundary elements with two local nodes were used for the discretization of the external and internal boundaries. In our numerical procedure, all boundaries (internal and external) are discretized only once.

In intersection points of boundary elements, in which there is a continuity of the normal flux density, only one global node is located. However, at the two boundary elements intersection point in which there is a discontinuity of the normal flux density, the double node technique must be used, i.e. two global nodes are located at such a point.

At the intersection points of several boundary elements, the correct approximation of the normal flux density imposes the use of the multiple node technique, i.e. at the intersection point of n boundary elements, n global nodes are located.

2.3 Local co-ordinate system of the boundary element

In this paper, the usual numerical integration along the single boundary element is totally substituted by analytical integration. That was the reason to introduce a boundary element local co-ordinate system (u, v) according to Figure 2. Local co-ordinates (u, v) of the point P are computed from its global co-ordinates (x, y) according to the following equations:

$$u = \frac{2}{\ell} \cdot [(x - x_M) \cdot (x_2 - x_M) + (y - y_M) \cdot (y_2 - y_M)] \quad (3)$$

$$v = \sqrt{(x - x_M)^2 + (y - y_M)^2 - u^2} \quad (4)$$

$$x_M = \frac{x_1 + x_2}{2} \quad ; \quad y_M = \frac{y_1 + y_2}{2} \quad (5)$$

where ℓ is the boundary element length, (x_1, y_1) are global co-ordinates of the local node 1 and (x_2, y_2) are global co-ordinates of the local node 2.

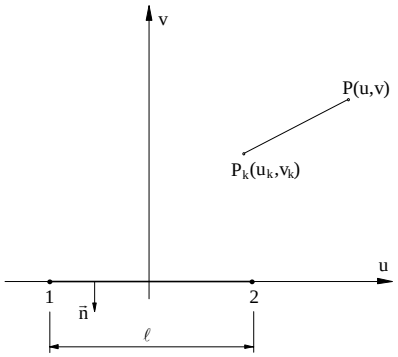

Fig. 2 Linear boundary element in the local co-ordinate system

For linear boundary elements, the potential distribution φ and the normal flux density q along the single boundary element are approximated by:

$$\Phi = \sum_{i=1}^{2} N_i \cdot \Phi_i \quad (6)$$

$$Q = \sum_{i=1}^{2} N_i \cdot Q_i \quad (7)$$

where N_i is the shape function joined to the *i-th* local node, Φ_i is the potential at the *i-th* node and Q_i is the

value of the normal component of the flux density at the *i-th* node.

The shape functions are defined in the local co-ordinate system (u, v) as follows:

$$N_1 = \frac{\ell - 2u}{2\ell} \tag{8}$$

$$N_2 = \frac{\ell + 2u}{2\ell} \tag{9}$$

For simplicity, the local nodes of each boundary element are positioned so that the normal always has the position as shown in Figure 2.

2.4 System of linear equations

Since the integration along the boundary curve $\Gamma_{pr} \backslash P_k$ is equal to sum of the integrals along all corresponding boundary elements, then, according to Eqs. (1), (6) and (7), the potential at the point P_k belonging to the *p-th* sub-domain is described by:

$$C_k \cdot \varphi_k = \sum_{r=1}^{NSD} a_{pr} \cdot \left\{ \sum_{j=1}^{NE} \left[\sum_{i=1}^{2} \left(\frac{1}{\kappa_p} \int_{\Gamma_{prj} \backslash P_k} \psi_k \cdot N_i \cdot d\Gamma \right) \cdot Q_i - \right. \right.$$
$$\left. \left. - \sum_{i=1}^{2} \left(\int_{\Gamma_{prj} \backslash P_k} N_i \cdot \frac{\partial \psi_k}{\partial n} \cdot d\Gamma \right) \cdot \Phi_i \right] \right\} \tag{10}$$

where NE is the total number of boundary elements in the whole domain Ω and Γ_{prj} is a part of the boundary Γ_{pr} belonging to the *j-th* boundary element.

The expression (10) in matrix notation can be written as:

$$C_k \cdot \varphi_k = \sum_{r=1}^{NSD} \sum_{j=1}^{NE} \sum_{i=1}^{2} \left(G^*_{kji} \cdot Q_i - H^*_{kji} \cdot \Phi_i \right) \tag{11}$$

where:

$$G^*_{kji} = a_{pr} \cdot \frac{1}{\kappa_p} \int_{\Gamma_{prj} \backslash P_k} \psi_k \cdot N_i \cdot d\Gamma \tag{12}$$

$$H^*_{kji} = a_{pr} \cdot \int_{\Gamma_{prj} \backslash P_k} N_i \cdot \frac{\partial \psi_k}{\partial n} \cdot d\Gamma \tag{13}$$

In our numerical procedure, the coefficients G^*_{kji} and H^*_{kji} are computed by analytical integration (Appendix A).

Using global nodes notation, the equation (11) can be written:

$$C_k \cdot \varphi_k = \sum_{m=1}^{NN} \left(G_{km} \cdot Q_m - H_{km} \cdot \Phi_m \right) \tag{14}$$

where NN is the total number of global nodes, Φ_m is the potential at the *m-th* global node and Q_m is the normal component of the flux density at the *m-th* global node.

The unknown potentials and normal densities at the global nodes can be computed using the point collocation method. It is useful to assume that the total number of collocation points is equal to the total number of unknowns. In other words, one collocation point per sub-domain is joined to each global node with at least one unknown.

If at a single point there is only one global node (single global node case), then the joined collocation point is located at observed node (Figure 3-a). If at a single point there are two global nodes (double global node case) or several global nodes (multiple global node case), then the joined collocation points are moved from the observed nodes along the associated boundary elements by one-quarter of the boundary element length (Figure 3-b). The system of linear equations obtained by this algorithm is regular in all cases.

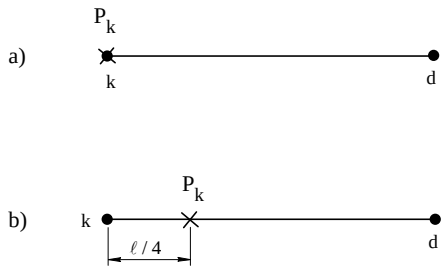

Fig. 3 Location of the collocation point P_k joined to the k-th node

Collocation point method, applied to Eq. (14), gives the next system of linear equations:

$$C_k \cdot (\alpha_k \cdot \Phi_k + \beta_k \cdot \Phi_d) = \sum_{m=1}^{NN} (G_{km} \cdot Q_m - H_{km} \cdot \Phi_m)$$
$$k = 1,2,...,NU \tag{15}$$

where NU is the total number of unknowns, Φ_k is *k-th* global node potential, Φ_d is *d-th* global node potential, while the values of the α_k and β_k are: $\alpha_k=1$; $\beta_k=0$ if the collocation point is located in the *k-th* global node; $\alpha_k=0.75$; $\beta_k=0.25$ if collocation point P_k is moved from the *k-th* node.

The system of linear equations (15) in matrix notation can be written as:

$$\boldsymbol{G} \cdot \boldsymbol{Q} - \boldsymbol{H} \cdot \boldsymbol{\Phi} = \boldsymbol{C} \cdot \boldsymbol{\Phi} \tag{16}$$

2.5 Additional equations

The system of linear equations (16) is regular. However, in points with more than one global node, the potential continuity, which must be satisfied, can be significantly interrupted. Therefore, from reason of numerical stability, the new equations have been added to this system. These additional equations equalize the potentials of the global nodes located in the same point.

So, for illustrative example presented in Figure 4, at the junction point of four sub-domains, the additional equations are:

$$\varphi_{100}=\varphi_{120} \quad (17)$$

$$\varphi_{100}=\varphi_{140} \quad (18)$$

$$\varphi_{100}=\varphi_{150} \quad (19)$$

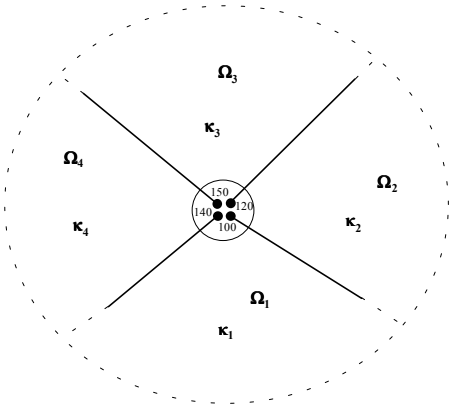

Fig. 4 Junction point of four sub-domains

2.6 Solution of linear algebric equations

The extended system of linear algebric equations can be written in the following form:

$$\boldsymbol{A}\cdot\boldsymbol{X}=\boldsymbol{B} \quad (20)$$

where $\boldsymbol{X}$ is the vector of unknowns.

By solving the system of linear equations (20), the unknown normal flux densities and potentials at all global nodes can be computed. In general case, this is situation when we wish to find the least-squares solution to an overdetermined set of linear equations. Since this set of equations is very close to singular, the system of equations (20) has been solved using the algorithm based on singular value decomposition [4].

3. NUMERICAL EXAMPLE

The method presented in this paper is applied to the stationary electric current field example with an analytical solution. Computational domain is heterogeneous and consists of four homogeneous sub-domains (Figure 5). Electric conductivity of sub-domains are $\kappa_1=\kappa_2=1$ *S/m* and $\kappa_3=\kappa_4=4$ *S/m*. Boundary conditions are: $\varphi=\varphi_a=100$ *V* on the boundary $y=0$ *m*, $\varphi=\varphi_b=0$ *V* on the boundary $y=1$ *m*, $q=0$ *A/m*^{2} on the boundaries $x=0$ *m* and $x=1$ *m*.

Since $\kappa_1=\kappa_2$ and $\kappa_3=\kappa_4$, for the given input data, the potential distribution is described by the following analytical expression:

$$\varphi=\begin{cases}100-160\cdot y \ \ [V] & \text{if} \quad 0\,m\le y\le 0.5\,m\\ 40\cdot(1-y) \ \ [V] & \text{if} \quad 0.5\,m\le y\le 1\,m\end{cases} \quad (21)$$

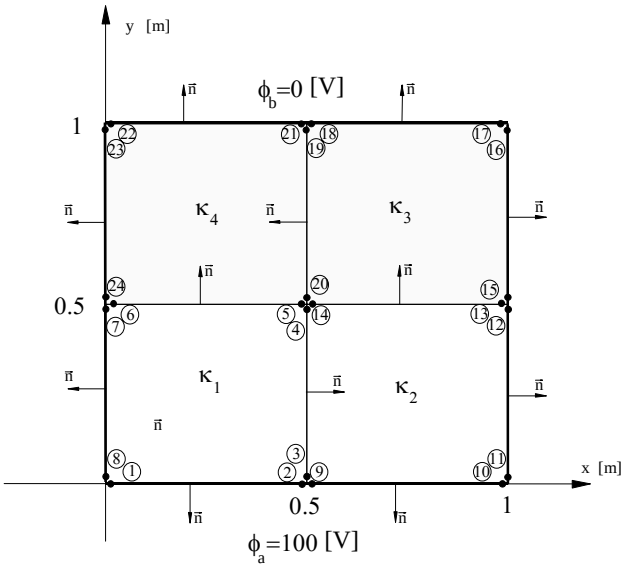

Fig. 5 Heterogeneous domain divided into four homogeneous sub-domains

The total number of boundary elements is *12* and the total number of global nodes is *24*. Co-ordinates of the global nodes are presented in Table 1, the prescribed values of the potentials and normal flux densities at the global nodes are presented in Table 2, and connection matrix is presented in Table 3. For this numerical example, numerical values of potentials and normal flux densities computed by developed BEM algorithm (Table 4) are exact.

Table 1 Co-ordinates of the global nodes

Key No.	x [m]	y [m]	Key No.	x [m]	y [m]
1	0	0	13	1	0.5
2	0.5	0	14	0.5	0.5
3	0.5	0	15	1	0.5
4	0.5	0.5	16	1	1
5	0.5	0.5	17	1	1
6	0	0.5	18	0.5	1
7	0	0.5	19	0.5	1
8	0	0	20	0.5	0.5
9	0.5	0	21	0.5	1
10	1	0	22	0	1
11	1	0	23	0	1
12	1	0.5	24	0	0.5

Table 2 Prescribed potentials and normal flux densities

Prescribed potentials		Prescribed normal flux densities	
Global node	φ [V]	Global node	Q [A/m^2]
1	100	7	0
2	100	8	0
9	100	11	0
10	100	12	0
17	0	15	0
18	0	16	0
21	0	23	0
22	0	24	0

Table 3 Connection matrix

Boundary Element	Local node 1	Local node 2	The first sub-domain	The second sub-domain
1	1	2	1	0
2	3	4	1	2
3	5	6	1	4
4	7	8	1	0
5	9	10	2	0
6	11	12	2	0
7	13	14	2	3
8	15	16	3	0
9	17	18	3	0
10	19	20	3	4
11	21	22	4	0
12	23	24	4	0

Table 4 Output data

Global node	φ [V]	Q [A/m^2]
1	100	160
2	100	160
3	100	0
4	20	0
5	20	-160
6	20	-160
7	20	0
8	100	0
9	100	160
10	100	160
11	100	0
12	20	0
13	20	-160
14	20	-160
15	20	0
16	0	0
17	0	-160
18	0	-160
19	0	0
20	20	0
21	0	-160
22	0	-160
23	0	0
24	20	0

4. CONCLUSIONS

The algorithm developed for 2D BEM analysis of potential Laplace problems has several advances. The first of them is the numerical integration along the linear boundary elements replaced by analytical integration. The second important advance is that singularity of the system of linear equations, which can be caused by the use of the double and multiple global node technique, has been avoided. It has been solved in such a way that the joined collocation points are moved from the points with more than one global node along the associated boundary elements by one-quarter of the boundary element length. Using double and multiple global node technique, the correct numerical approximation of the normal flux density at the points with its physically discontinuity has been made possible. However, the numerical approximation of the potential is correct if potential continuity at all points is satisfied. For this reason, a new set of linear equations has been added to the regular system of linear equations. These additional equations equalize the potentials of the global nodes located in the same point. However, for real problems, the both basic and extended systems of linear equations are very close to singular due to ill-conditioned matrices. Therefore, the extended system of equations has been solved using the algorithm based on singular value decomposition [4].

5. APPENDIX A

The exact analytical expressions for coefficients G^*_{kji} and H^*_{kji}, described by Eqs. (12) and (13), have been obtained by analytical integration along boundary element using its local co-ordinate system (Figure 2). Regarding the collocation point location there are five possibilities:

a) The collocation point does not belong to the j-th boundary element:

$$G^*_{kj1} = -\frac{1}{4\pi\kappa_p \ell}\cdot\left\{\left(\frac{\ell}{2}-u_k\right)\cdot\left[I_1\left(u_k-\frac{\ell}{2}\right)-I_1\left(u_k+\frac{\ell}{2}\right)\right]+\right.$$
$$\left.+\left[I_2\left(u_k-\frac{\ell}{2}\right)-I_2\left(u_k+\frac{\ell}{2}\right)\right]\right\}+\frac{1}{2\kappa_p}\cdot A\cdot\ell \qquad \text{(A1)}$$

$$G^*_{kj2} = -\frac{1}{4\pi\kappa_p \ell}\cdot\left\{\left(\frac{\ell}{2}+u_k\right)\cdot\left[I_1\left(u_k-\frac{\ell}{2}\right)-I_1\left(u_k+\frac{\ell}{2}\right)\right]-\right.$$
$$\left.-\left[I_2\left(u_k-\frac{\ell}{2}\right)-I_2\left(u_k+\frac{\ell}{2}\right)\right]\right\}+\frac{1}{2\kappa_p}\cdot A\cdot\ell \qquad \text{(A2)}$$

$$H^*_{kj1} = p\cdot\frac{v_\kappa}{2\pi\ell}\cdot\left\{\left(\frac{\ell}{2}-u_k\right)\cdot\left[I_3\left(u_k-\frac{\ell}{2}\right)-I_3\left(u_k+\frac{\ell}{2}\right)\right]+\right.$$
$$\left.+\left[I_4\left(u_k-\frac{\ell}{2}\right)-I_4\left(u_k+\frac{\ell}{2}\right)\right]\right\} \qquad \text{(A3)}$$

$$H^*_{kj2} = p\cdot\frac{v_\kappa}{2\pi\ell}\cdot\left\{\left(\frac{\ell}{2}+u_k\right)\cdot\left[I_3\left(u_k-\frac{\ell}{2}\right)-I_3\left(u_k+\frac{\ell}{2}\right)\right]-\right.$$
$$\left.-\left[I_4\left(u_k-\frac{\ell}{2}\right)-I_4\left(u_k+\frac{\ell}{2}\right)\right]\right\} \qquad \text{(A4)}$$

where:

$$I_1 = \int ln(t^2+v_k^2)\cdot dt = \qquad \text{(A5)}$$
$$= t\cdot ln(t^2+v_k^2) - 2\cdot t + 2\cdot v_k\cdot arctg\frac{t}{v_k}$$

$$I_2 = \int t\cdot ln(t^2+v_k^2)\cdot dt = \qquad \text{(A6)}$$
$$= \frac{1}{2}\cdot(t^2+v_k^2)\cdot ln(t^2+v_k^2) - \frac{t^2}{2}$$

$$I_3 = \int\frac{dt}{t^2+v_k^2} = \frac{1}{v_k}\cdot arctg\frac{t}{v_k} \qquad \text{(A7)}$$

$$I_4 = \int\frac{tdt}{t^2+v_k^2} = \frac{1}{2}\cdot ln(t^2+v_k^2) \qquad \text{(A8)}$$

$$I_5 = \int ln\,t\,dt = t\cdot(ln\,t-1) \qquad \text{(A9)}$$

$$I_6 = \int t \ln t dt = \frac{t^2}{2} \cdot (\ln t - \frac{1}{2}) \qquad \text{(A10)}$$

$$p = sign\left[(x_k - x_1)\cdot(y_2 - y_1) + (y_k - y_1)\cdot(x_1 - x_2)\right] \qquad \text{(A11)}$$

while (x_k, y_k) are global co-ordinates of the collocation point P_k; (x_1, y_1) are global co-ordinates of the local node 1 and (x_2, y_2) are global co-ordinates of the local node 2.

b) P_k is located in the local node 1 of the j-th boundary element:

$$G^*_{kj1} = \frac{1}{2\pi\kappa_p \ell}\cdot\left[I_6(\ell) - \ell\cdot I_5(\ell)\right] + \frac{1}{2\kappa_p}\cdot A\cdot\ell \qquad \text{(A12)}$$

$$G^*_{kj2} = -\frac{1}{2\pi\kappa_p \ell}\cdot I_6(\ell) + \frac{1}{2\kappa_p}\cdot A\cdot\ell \qquad \text{(A13)}$$

$$H^*_{kj1} = H^*_{kj2} = 0 \qquad \text{(A14)}$$

c) P_k is located in the local node 2 of the j-th boundary element:

$$G^*_{kj1} = -\frac{1}{2\pi\kappa_p \ell}\cdot I_6(\ell) + \frac{1}{2\kappa_p}\cdot A\cdot\ell \qquad \text{(A15)}$$

$$G^*_{kj2} = \frac{1}{2\pi\kappa_p \ell}\cdot\left[I_6(\ell) - \ell\cdot I_5(\ell)\right] + \frac{1}{2\kappa_p}\cdot A\cdot\ell \qquad \text{(A16)}$$

$$H^*_{kj1} = H^*_{kj2} = 0 \qquad \text{(A17)}$$

d) P_k is moved from the local node 1 along the j-th boundary element:

$$G^*_{kj1} = -\frac{1}{2\pi\kappa_p \ell}\cdot \cdot\left[\frac{3\ell}{4} I_5\left(\frac{3\ell}{4}\right) + \frac{3\ell}{4} I_5\left(\frac{\ell}{4}\right) - I_6\left(\frac{3\ell}{4}\right) + I_6\left(\frac{\ell}{4}\right)\right] + \frac{1}{2\kappa_p}\cdot A\cdot\ell \qquad \text{(A18)}$$

$$G^*_{kj2} = -\frac{1}{2\pi\kappa_p \ell}\cdot \cdot\left[\frac{\ell}{4} I_5\left(\frac{3\ell}{4}\right) + \frac{\ell}{4} I_5\left(\frac{\ell}{4}\right) + I_6\left(\frac{3\ell}{4}\right) - I_6\left(\frac{\ell}{4}\right)\right] + \frac{1}{2\kappa_p}\cdot A\cdot\ell \qquad \text{(A19)}$$

$$H^*_{kj1} = H^*_{kj2} = 0 \qquad \text{(A20)}$$

e) P_k is moved from the local node 2 along the j-th boundary element:

$$G^*_{kj1} = -\frac{1}{2\pi\kappa_p \ell}\cdot \cdot\left[\frac{\ell}{4} I_5\left(\frac{3\ell}{4}\right) + \frac{\ell}{4} I_5\left(\frac{\ell}{4}\right) + I_6\left(\frac{3\ell}{4}\right) - I_6\left(\frac{\ell}{4}\right)\right] + \frac{1}{2\kappa_p}\cdot A\cdot\ell \qquad \text{(A21)}$$

$$G^*_{kj2} = -\frac{1}{2\pi\kappa_p \ell}\cdot \cdot\left[\frac{3\ell}{4} I_5\left(\frac{3\ell}{4}\right) + \frac{3\ell}{4} I_5\left(\frac{\ell}{4}\right) - I_6\left(\frac{3\ell}{4}\right) + I_6\left(\frac{\ell}{4}\right)\right] + \frac{1}{2\kappa_p}\cdot A\cdot\ell \qquad \text{(A22)}$$

$$H^*_{kj1} = H^*_{kj2} = 0 \qquad \text{(A23)}$$

6. REFERENCES

[1] L. Bruch and A. Lajeune, An effective solution of the numerical problems at multi-domain points for anisotropic Laplace problems, In: C.A. Brebbia and J.J. Connor (editors), Advances in Boundary Elements, Vol. 2, Field and Fluid Flow Solutions, Springer-Verlag, Berlin, 1989.

[2] M. Kurtović and S. Vujević, Earthing grid parameters with conductor surrounded by an additional substance, *IEE Proceedings Generation, Transmission and Distribution*, Vol. 147, No. 1, pp. 57-61, 2000.

[3] C.A. Brebbia and S. Walker, *Boundary Element Techniques in Engineering*, Newnes-Butterworths, London-Boston, 1980.

[4] W.H. Press, S.A. Teukolsky, W.T. Vetterling and B.P. Flanerry, *Numerical Recipes in FORTRAN - The Art of Scientific Computing* - Second Edition, Cambridge University Press, New York, 1992.

DVODIMENZIONALNI PRORAČUN RASPODJELE POTENCIJALA OPISANIH LAPLACE-OVOM JEDNADŽBOM METODOM RUBNIH ELEMENATA

SAŽETAK

U radu je opisan algoritam za proračun raspodjele potencijala u ravnini (2D) metodom rubnih elemenata (BEM) i to za probleme opisane Laplace-ovom jednadžbom, dok je područje proračuna heterogeno. Uporabom tehnike dvostrukih i višestrukih globalnih čvorova, moguće je dobiti fizikalno ispravno rješenje za normalnu komponentu gustoće toka i u točkama u kojima postoji njen diskontinuitet. Osim toga, osnovni sustav linearnih jednadžbi je nadopunjen novim skupom linearnih jednadžbi koje izjednačavaju potencijale globalnih čvorova smještenih u istoj točki. Točnost proračuna je dodatno povećana uporabom novih izraza dobivenih analitičkom integracijom duž linearnih graničnih elemenata. Uporabom razvijenog numeričkog algoritma riješen je pokazani primjer koji ima poznato analitičko rješenje.

***Ključne riječi**: 2D BEM analiza, Laplace-ova jednadžba, analitička integracija, tehnika višestrukih globalnih čvorova.*